Mass Spectroscopy of Chemical Reaction of 3d Metal Clusters Involved in Chemical Vapor Deposition Synthesis of Carbon Nanotubes

Shuhei Inoue* and Shigeo Maruyama[†]

Department of Mechanical Engineering, The University of Tokyo, 7-3-1 Hongo, Bunkyo-ku, Tokyo 113-8656, Japan

The chemical reactions of transition metal clusters in the gas phase have aroused considerable scientific interest and are also of critical scientific importance. For example, these reactions are involved in the synthesis of single-walled carbon nanotubes, which are considered ideal materials because of their outstanding properties. Alcohol catalytic chemical vapor deposition (ACCVD) is one of the best synthetic processes for carbon nanotubes (CNTs); however, even the initial growth mechanism is still unclear, unlike those of other synthetic processes. In this study, we used a Fourier transform ion cyclotron resonance (FT-ICR) mass spectrometer to determine the initial reactions of transition metal cluster ions (iron, cobalt, and nickel) that are typically adopted in the alcohol CVD process. Metal clusters with approximately 10–25 atoms each, generated by a pulsed laser ablation system in a supersonic-expansion cluster beam source, were directly carried into the FT-ICR cell. Subsequently, ethanol was introduced into the ICR cell. We observed two different results: one was simple chemisorption observed in the iron cluster and the other was dehydrogenated chemisorption observed in the nickel cluster; however, cobalt clusters exhibited both patterns, and a sequential reaction was observed. Furthermore, the dehydrogenation of ethanol on the cobalt cluster is fully described from isotope-labeled experiments.

KEYWORDS: cluster, iron, cobalt, nickel, FT-ICR, single-walled carbon nanotubes

---

*Present address: Department of Mechanical System Engineering, Hiroshima University, 1-4-1 Kagamiyama, Higashi-Hiroshima, Hiroshima 739-8527, Japan.

[†]E-mail address: maruyama@photon.t.u-tokyo.ac.jp.

1. Introduction

Carbon nanotubes (CNTs), [1] which were discovered in 1991, are classified into two types: single-walled carbon nanotubes (SWNTs) [2] and multi-walled carbon nanotubes (MWNTs). [1] It is expected that CNTs can be used as novel materials owing to their various outstanding physical and chemical characteristics. Thus far, a considerable number of attempts to apply SWNTs to field-effect transistors, [3, 4] atomic force microscope tips, [5, 6] nanocomposite, [7] and field emitters [8, 9] have been reported.

With regard to the apparatus and costs, the chemical vapor deposition (CVD) method is currently regarded as the most reasonable technique for the industrial or commercial production of SWNTs. [10–15] The high-pressure CO (HiPco) method, [16] is recognized as a commercially feasible approach to continuously produce large amounts of relatively high-quality SWNTs. Recently, Maruyama *et al.* [17] proposed a new CVD method in which, for the first time, alcohols (e.g., ethanol and methanol) were employed as the carbon source for the synthesis of SWNTs. This method, called the alcohol catalytic CVD (ACCVD) method, is better than the other CVD methods because it can produce high-quality SWNTs at relatively low temperature. However, its growth mechanism has not been clarified; therefore, fundamental investigations on the growth mechanism are essential for the further improvement of the ACCVD method. In the CVD method, transition metals such as Fe, Ni, and Co are used as catalysts. On the other hand, there are a large number of studies being conducted on these clusters in the gas phase. [18–24] However, most of the present research is restricted to small clusters (less than 10 atoms) because the generation of large clusters is quite difficult. Generally, in a catalytic reaction, because a certain number of atoms or a local structure of a small particle has a catalytic activity, clusters with less than 10 atoms are slightly insufficient for specifying the catalytic reaction. Furthermore, the size of catalysts employed in CVD synthesis of SWNTs is approximately 0.5 nm to 4 nm. Calculating from the bulk density, there are approximately 50 atoms in a 1-nm-diameter spherical particle. Usually, a particle with less than 100 atoms does not have a bulk crystal structure but an atomic cluster structure. Thus, there should be less than 50 atoms in a 1-nm-particle and less than about 20 atoms in a 0.75-nm-diameter particle. In this report, we explored the basic reaction mechanism of large-size clusters (Fe, Co, and Ni) with 10 – 30 atoms at room temperature; consequently, cobalt clusters with 12 –17 atoms showed a unique reaction. Although the reaction temperature is different from the practical ACCVD process, the reaction mechanism derived in this study can be a possible candidate.

2. Experimental Procedure

Our experimental apparatus was based on the same design concept as that of the apparatus used by Smalley's group, [25] the detailed characteristics of which are

described elsewhere. [26–29] Figures 1 and 2 show the cluster beam source and the direct-injection Fourier-transform ion cyclotron resonance (FT-ICR) apparatus, respectively. The metal cluster ion beam was generated outside a magnetic field using the laser-vaporization cluster beam source, as shown in Fig. 1. A pulsed gas valve, the sample motion mechanism, and a skimmer were installed in a 6-in six-way ultra high vacuum (UHV) cross. A solid sample disk was vaporized by a focused beam from an Nd:YAG laser (second harmonics) while the timed pulsed gas was injected into the nozzle. In a helium gas atmosphere, the vaporized atoms condensed into clusters and were then carried and cooled by the supersonic expansion of helium gas. The cluster beam was directly injected into the magnetic field through the skimmer with an opening diameter of 2 mm and a deceleration tube.

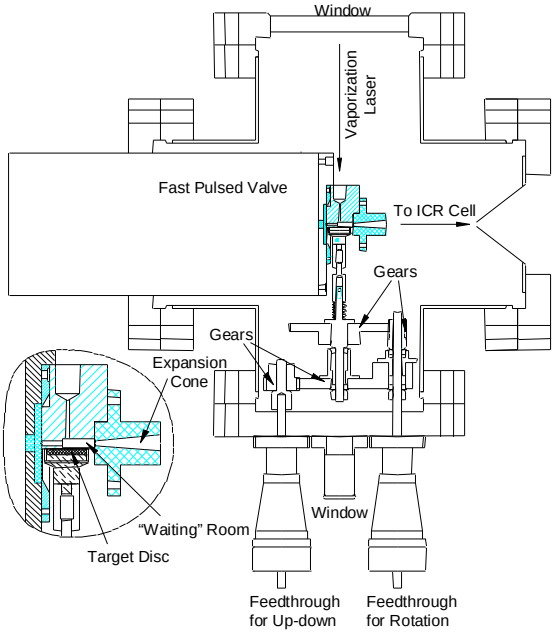

Fig. 1. Laser-vaporization cluster beam source.

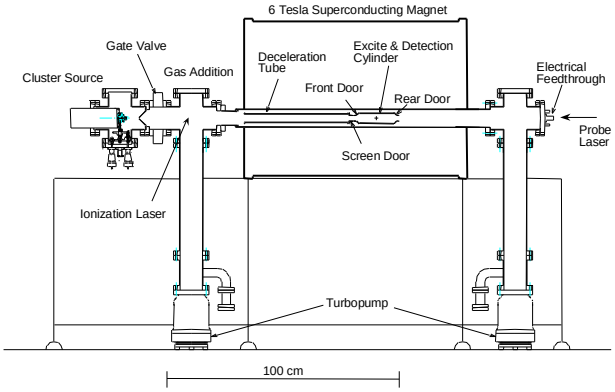

Fig. 2. FT-ICR apparatus with direct injection cluster beam source.

FT-ICR is a unique mass spectroscopy technique based on the ion-cyclotron motion of cluster ions in a strong magnetic field. The ion-cyclotron frequency f is inversely proportional to the ion mass M as follows.

$$f = \frac{qB}{2\pi M} \quad (1)$$

An extremely high mass resolution at a high mass range, such as the resolution of 1 amu in a 10,000 amu range, can be obtained. Furthermore, because the ions can be trapped in a vacuum for a few minutes, it is possible to perform chemical reaction experiments. The ICR cell used was a cylinder with a length and internal diameter of 150 and 42 mm, respectively. It was placed in a stainless-steel tube (SUS316) with an internal diameter of 84 mm, which penetrated a homogeneous 5.83 T superconducting magnet that is commercially available for a nuclear magnetic resonance (NMR) apparatus. Two turbomolecular pumps (300 L/s) fore-pumped by a smaller one of 50 L/s were placed on the floor in order to avoid the effect of the strong magnetic field. The typical background pressure was 3×10^{-10} Torr.

For the chemical reaction experiments, ethanol gas was supplied to the ICR cell for a certain period through the pulsed valve, which was adjusted to maintain the pressure of the ICR cell at approximately 1×10^{-8} Torr. After the reaction experiment, the cluster ions were excited to detect their mass distribution.

3. Results and Discussion

3.1 *Simple chemisorption of ion clusters*

Figure 3(a) shows the typical spectrum of the "as-injected" iron clusters. The bottom and top axes denote the mass of the clusters in amu and the number of iron atoms, respectively. Because iron has four natural isotopes, each spectrum peak also has some width. The very small peaks shown between each iron cluster peak in Fig. 3(a) are iron clusters with water molecule, which inevitably exists in the gas line. As shown in Fig. 3(b), the reaction products appeared just behind the bare iron cluster spectra after a 2 s reaction at 1×10^{-8} Torr with ethanol-d_3 (CD_3CH_2OH). Figure 4(a) shows an expanded view of the portion indicated by the square in Fig. 3(b), and Fig. 4(b) is the isotope distribution of Fe_{11} calculated from the natural abundance of isotopes. These isotope distributions show quite good agreement with each other, in comparison with their proportions labeled as ▲, ■, ●, and ○, respectively. In this reaction, ethanol-d_3 was used as the reaction gas, and the mass difference between the original clusters and reaction products, the isotropic mass distribution of which showed good agreement with the bare iron cluster, was 49 amu, which is the mass of ethanol-d_3; thus, each component of ethanol-d_3 was simply chemisorbed on the iron clusters. In this paper, we name this reaction "simple chemisorption."

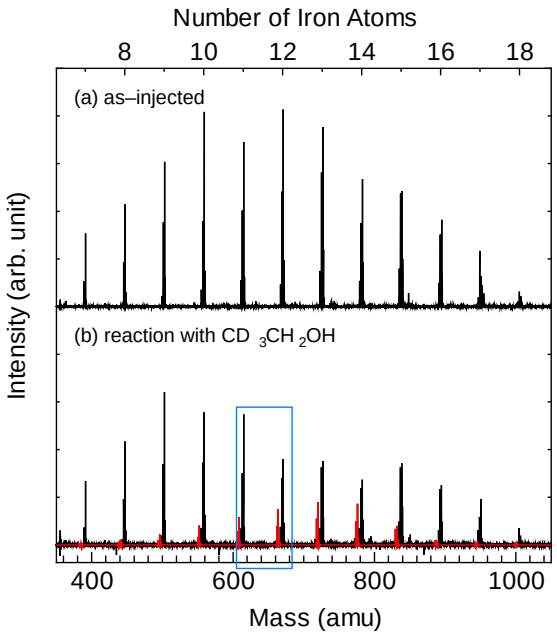

Fig. 3. (Color online) Chemical reaction of iron clusters with ethanol-d_3.

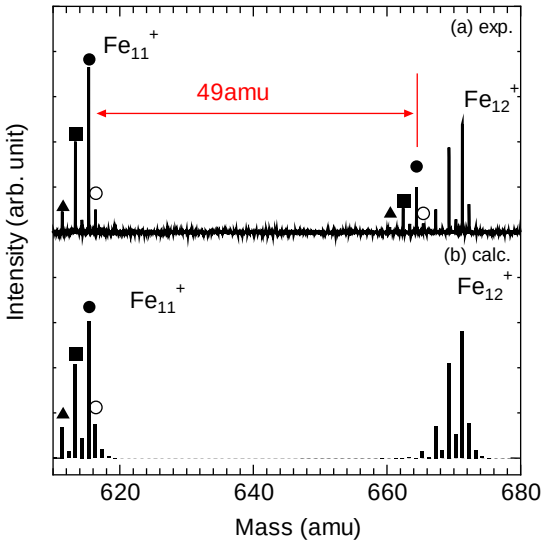

Fig. 4. Chemical reaction of iron clusters with ethanol-d_3. (a) is the expanded view of Fig. 3(b) and (b) is the simulated spectrum based on the natural abundance of isotopes.

3.2 *Dehydrogenated chemisorption of nickel clusters*

Figure 5(A-a) shows the typical mass spectrum of the as-injected nickel clusters. A small amount of water molecules chemisorbed on the nickel clusters. In this figure, the bottom axis represents the mass in amu, and the number of nickel atoms is represented by the top axis. Because nickel has five natural isotopes, each spectrum also has some width; moreover, the measured isotope distribution is quite consistent with the calculation based on the natural abundance of isotopes. Figures 5(A-b) and 5(A-c) show the results of the reaction experiments with normal ethanol (CH_3CH_2OH) (1 s at 1×10^{-8}

Torr) and ethanol-d_3 (1 s at 1×10^{-8} Torr), respectively. In these results, each reaction product appeared just behind the next bared nickel cluster; hence, the chemisorptions were expected to be quite similar to those in the case of the iron clusters. Figures 5(B) and 5(C) are the expanded views of Figs. 5(A-b) and 5(A- c). In the case of Fig. 5(B), the mass gap between the reaction product and the original bare nickel clusters is 42 amu; thus, it is considered that four hydrogen atoms were dissociated and detached. In the case of Fig. 5(C), because the mass gap is 43 amu, two hydrogen atoms and two deuterium atoms must be dissociated and detached. In this paper, we name this reaction "dehydrogenated chemisorption."

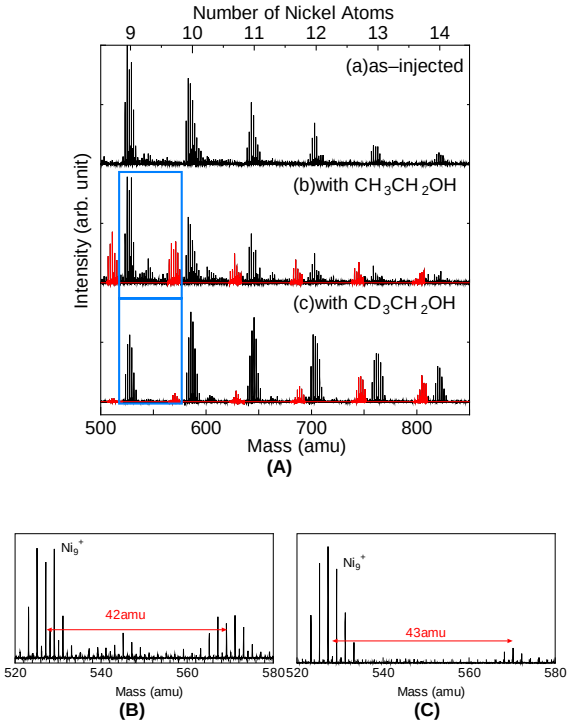

Fig. 5. (Color online) Chemical reactions of nickel clusters with ethanol. A(a) is as injected spectrum, A (b) is reaction with normal ethanol (CH_3CH_2OH), and A-(c) is reaction with isotopic ethanol (CD_3CH_2OH). B and C are expanded views of those indicated by square frames in A(b) and A(c), respectively.

3.3 *Simple and dehydrogenated chemisorption of cobalt clusters*

Figure 6(a) shows the typical mass spectrum of the as-injected cobalt clusters. The upper axis denotes the number of cobalt atoms and the bottom axis, the mass in amu. Cobalt has no naturally occurring isotopes and, hence, its spectrum is very simple. The small peaks between the strong peaks of the cobalt clusters indicate the cobalt clusters with one water molecule each; water invariably exits in the ICR cell, cluster beam source, and helium gas. Figures 6(b)–6(d) show the results of the reaction

experiments with ethanol for 0.2, 0.5, and 1.0 s with ethanol pressure at 1×10^{-8} Torr. Mainly two types of reaction pattern depending on cluster size are observed as in Fig. 6(c). In the case of Co_n^+ ($n < 12$, $n > 17$), simple chemisorption is observed, and in case of Co_n^+ ($12 \le n \le 17$), both simple and dehydrogenated chemisorption are observed. This versatile reactivity could be related to the fact that cobalt is a generally better catalyst than iron and nickel for ACCVD. To understand this reaction, it is important to determine which hydrogen atoms dissociated in the dehydrogenated chemisorptions.

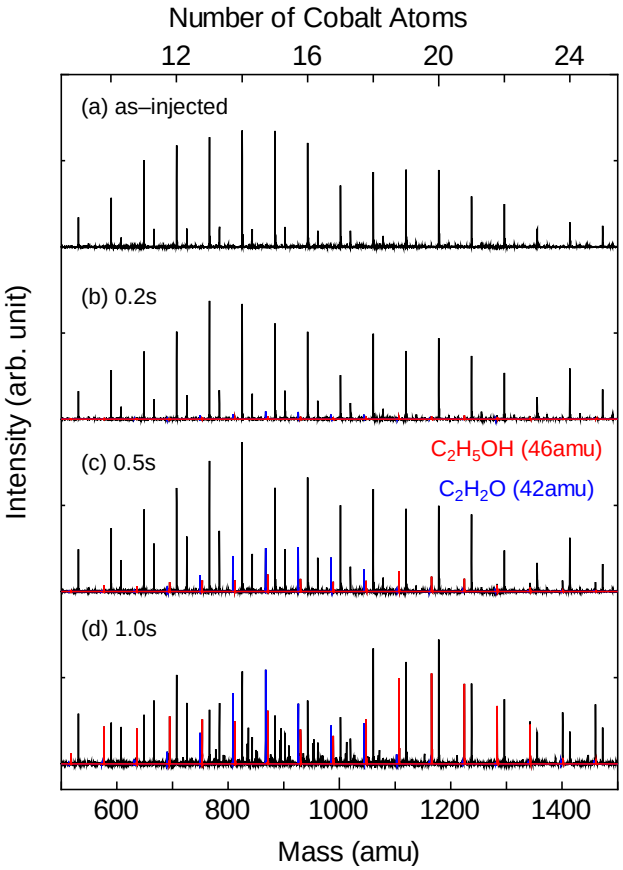

Fig. 6. (Color online) Chemical reaction of cobalt clusters with ethanol. (a) is as-injected mass spectrum and the values shown in (b) – (d) indicate the reaction time.

3.4 *Determination of hydrogen dissociation path for cobalt clusters*

To specify the dissociated hydrogen atoms, we employed isotopically labeled ethanol, ethanol-*d* (CH_3CH_2OD) in Fig. 7(b), ethanol-d_3 (CD_3CH_2OH) in Fig. 7(c), and ethanol-d_6 (CD_3CD_2OD) in Fig. 7(d) and we compared the mass spectra with that of normal ethanol shown in Fig. 7(a). In Fig. 7(a), we can easily assign that two strong signals: one is shown at approximately 42 amu from Co_{14}^+ (labeled ▼) and the other at approximately 46 amu (labeled ■), are dehydrogenated and simple chemisorptions, respectively. Assuming that the reaction process itself does not depend on the isotopic

composition of ethanol, we can expect only two peaks of reaction products even for Figs. 7(b)-7(d). In Figs. 7(b)-7(d), dehydrogenated and simple chemisorptions peak are indicated by ▼ and ■, respectively. However, unlike Fig. 7(a), the mass peaks of reaction products are more complicated in Figs. 7(b) and 7(d). Several peaks in between these peaks with a mass separation of 1 amu can be explained by the exchange of hydrogen and deuterium on cobalt clusters in Appendix A.

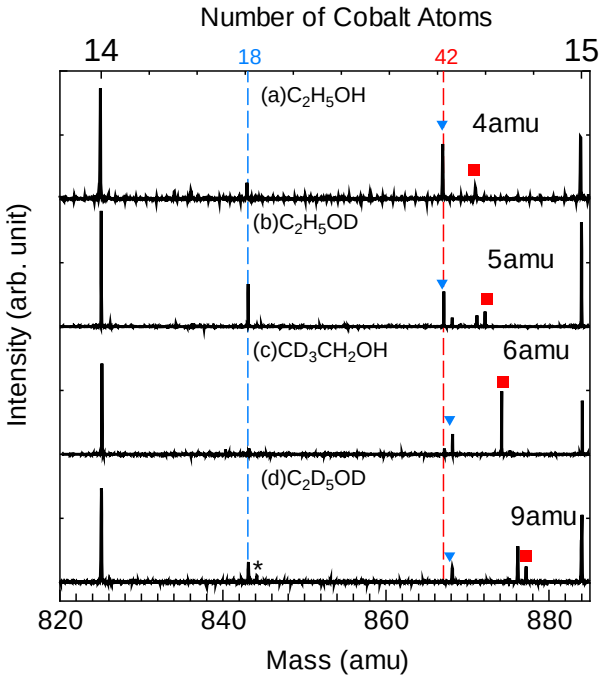

Fig. 7. (Color online) Chemical reactions of Co_{14}^{+} with isotopic ethanol. The values of 18 and 42 indicate the mass gaps in the atomic mass unit from the Co_{14}^{+} cluster. The symbols "▼" and "■" indicate spectra of simple chemisorptions and dehydrogenated chemisorptions, respectively. Captions in this figure (e.g., 4 and 5 amu) indicate the mass differences between simple chemisorptions and dehydrogenated chemisorptions.

Simple reaction pattern from ethanol-d_3 (CD_3CH_2OH) in Fig. 7(c) is useful for determining which hydrogen atoms in the original ethanol are detached. The dehydrogenated peak marked by ▼ is 43 amu from the bare Co_{14} cluster; hence one hydrogen and one deuterium should remain. Considering the original structure CD_3CH_2OH, the structure of the dehydrogenated molecule must be CD-CH-O. Thus, we can conclude that a hydrogen atom from OH, one hydrogen atom from C1, and two hydrogen atoms from C2 has detached as shown in Fig. 8(c). Here, we label a carbon atom next to OH as C1 and another carbon atom as C2. A further detailed study of ethanol-d_3 reaction summarized in Appendix B shows that a short-life-time intermediate state exists where only two hydrogen atoms detach. This intermediate state shown in

Fig. 8(b) is a loss of a hydrogen atom from OH and C2 each. Hence, the dehydrogenation sequence can be expressed as follows: a hydrogen atom in OH dissociates as ethanol chemisorbed to the Co cluster as in Fig. 8(a); a hydrogen atom from C2 dissociates and detaches the cluster as H_2 combined with the previous hydrogen atom as in Fig. 8(b); two hydrogen atoms from C1 and C2 dissociate and detach as H_2 as in Fig. 8(c). Consistency of this model with other isotope labeled experiments in Figs. 7(b) and 7(c) is confirmed in Appendix A. This reaction process should be a good benchmark for future quantum chemical simulations.

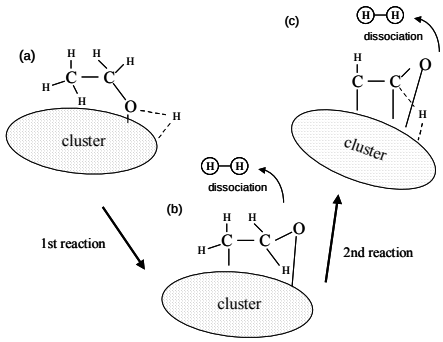

Fig. 8. Dehydrogenated chemisorptions. In the case of dehydrogenated chemisorptions, hydrogen atoms labeled "*1" dissociate first and those labeled "*2" dissociate next.

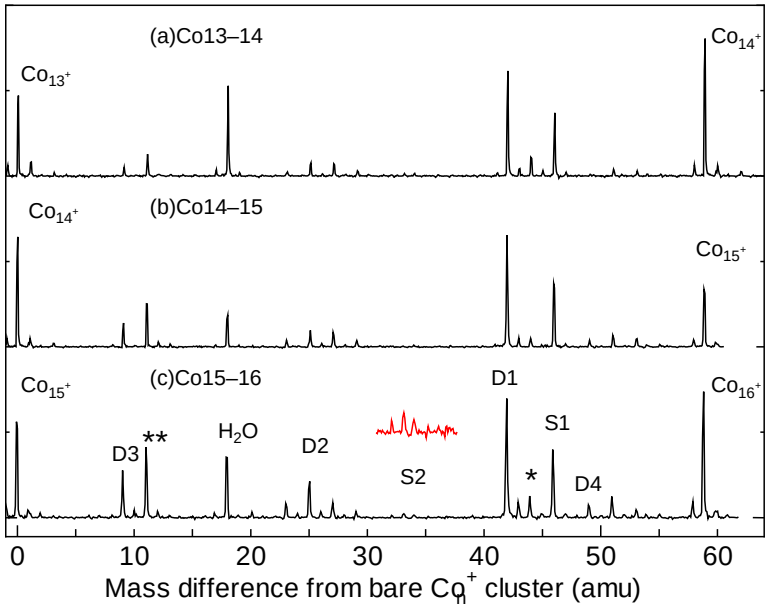

Fig. 9. Sequential reactions of Co_n^+ (n=13, 14, 15) with ethanol. Further reaction products are shown unlike in the case of iron and nickel clusters. Each labeled spectrum indicates a correspondent spectrum (D3: 3 ethanol molecules dehydrogenated chemisorptions).

3.5 *Further reaction of more ethanol molecules on a cobalt cluster*

A further reaction process with more than one ethanol molecule is studied with a longer reaction time of 2 s at 1×10^{-8} Torr in Fig. 9. Here, reaction products are compared for Co_{13}^{+}, Co_{14}^{+}, and Co_{15}^{+}. The spectrum patterns in Figs. 9(a)–9(c) are completely similar; hence, almost all of these signals are considered as those of reaction products and not noise, even if they are very weak. The label in Fig. 9(c) indicates the assigned reaction for each product. "S" and "D" denote "simple chemisorptions" and "dehydrogenated chemisorptions", respectively. A number after "S" or "D" is the number of reacted ethanol molecules. Peaks marked with "*" and "**" are intermediate H_2 dehydration and diethylether-like products ($C_2H_3OH_3C_2$), respectively. Table I shows experimentally derived and calculated values of the mass difference from the Co_{15}^{+} cluster. As shown in Table 1, a sequential reaction clearly occurred, but the mass differences of D3 and D4 are not completely consistent with the calculated values. Perhaps, owing to an increase in the number of reactant species, some interactions occurred among the reactants themselves, which brought about hydrogen adduction or non-detachment.

Table I Assignments of reaction products shown in Fig. 9(c).

Number of reactant	1	2	3	4	1	2
Product formula	Co_{15} (C_2H_2O)	Co_{14} $(C_2H_2O)_2$	Co_{13} $(C_2H_2O)_3$	Co_{13} $(C_2H_2O)_4$	Co_{15} (C_2H_6O)	Co_{14} $(C_2H_6O)_2$
Difference (exp.)	42.02	25.03	*9.07*	*50.96*	46.05	33.14
Difference (calc.)	42.01	25.08	*8.17*	*50.18*	46.04	33.14
Assignment	D1	D2	D3	D4	S1	S2

We cannot observe more than three "simple chemisorptions," S3, and S2 is already very weak in contrast to the clear signals of D3 and D4. We assume that there are two distinct isomers in small Co clusters. One isomer cluster is simple saturated with two "simple chemisorption" ethanol as shown in Fig. 10(a) and no further reaction is expected. The other isomer cluster can efficiently dissociate hydrogen until at least four ethanol molecules attach as shown in Fig. 10(b).

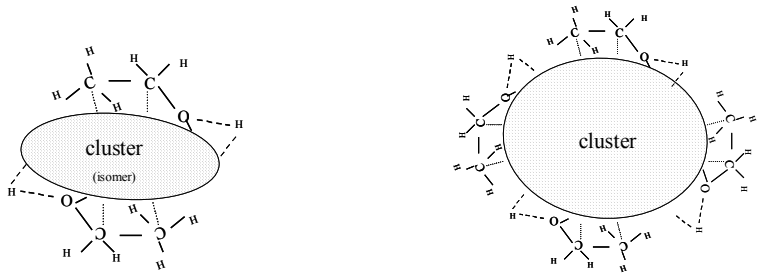

saturation sequential

Fig. 10. Schematic of reaction sites for cobalt cluster.

4. Conclusions

In this work, the chemical reactions of iron, cobalt, and nickel clusters with ethanol were studied. Iron and nickel clusters exhibited a single reaction pattern: either simple chemisorption or dehydrogenated chemisorption. On the other hand, cobalt clusters exhibited both reaction patterns depending on the cluster size, and furthermore, sequential reactions also occurred, unlike in the case of the iron and nickel clusters. This sequential reaction may bring about nucleation of SWNTs by further resolving ethanol molecules in the alcohol catalytic CVD (ACCVD) process.

ACKNOWLEDGMENT

Part of this work was financially supported by Grants-in-Aid for Scientific Research (19206024 and 19054003) from the Japan Society for the Promotion of Science (JSPS) and SCOPE (051403009) from the Ministry of International Affairs and Communications. S. Inoue was financially supported by a fellowship from JSPS.

References

1) S. Iijima: Nature **354** (1991) 56.
2) S. Iijima and T. Ichihashi: Nature **363** (1993) 603.
3) S. J. Tans, M. H. Devoret, H. J. Dai, A. Thess, R. E. Smalley, L. J. Geerligs, and C. Dekker: Nature **474** (1997) 386.
4) M. Bockrath, D. H. Cobden, P. L. McEuen, N. G. Chopra, A. Zettl, A. Thess, and R. E. Smalley: Science **275** (1997) 1922.
5) H. J. Dai, J. H. Hafner, A. G. Rinzler, D. T. Colbert, and R. E. Smalley: Nature **384** (1996) 147.
6) H. Nishijima, S. Kamo, S. Akita, Y. Nakayama, K. I. Hohmura, S. H. Yoshimura, and K. Takeyasu: Appl. Phys. Lett. **74** (1999) 4061.

7) B. I. Yakobson, M. P Campbell, C. J. Brabec, and J. Bernholc: Comput. Mater. Sci. **8** (1997) 341.
8) W. A. de Heer, A. Chatelain, and D. Ugarte: Science **270** (1995) 1179.
9) Y. Saito and U. Mori: Jpn. J. Appl. Phys. **37** (1998) 346.
10) H. J. Dai, A. Rinzler, P. Nikolaev, A. Thess, D. T. Colbert, and R. E Smalley: Chem. Phys. Lett. **260** (1996) 471.
11) H. M. Cheng, F. Li, G. Su, H.-Y. Pan, L. -L. He, X. Sun, and M. S. Dresselhaus: Appl. Phys. Lett. **72** (1998) 3282.
12) K. Mukhopadhyay, A. Koshio, T. Sugai, N. Tanaka, H. Shinohara, Z. Konya, and J. B. Nagy: Chem. Phys. Lett. **303** (1999) 117.
13) A. M. Rao, E. Richter, S. Bandow, B. Chase, P. C. Eklund, K. A. Williams, S. Fang, K. R. Subbaswamy, M. Menon, A. Thess, R. E. Smalley, G. Dresselhaus, and M. S. Dresselhaus: Science **275** (1997) 187.
14) M. Yudasaka, R. Yamada, N. Sensui, T. Wilkins, T. Ichihashi, and S. Iijima: J. Phys. Chem. B **103** (1999) 6224.
15) H. Kataura, Y. Kumazawa, Y. Maniwa, Y. Ohtsuka, R. Sen, S. Suzuki, and Y. Achiba: Carbon **38** (2000) 1691.
16) P. Nikolaev, M. J. Bronikowski, R. K. Bradley, F. Rohmund, D. T. Colbert, K. A. Smith, and R. E. Smalley: Chem. Phys. Lett. **313** (1999) 91.
17) S. Maruyama, R. Kojima, Y. Miyauchi, S. Chiashi, and M. Kohno: Chem. Phys. Lett. **360** (2002) 229.
18) Å. M. L. Øiestad and E. Uggerud: Chem. Phys. **262** (2000) 169.
19) J. Conceicao, R. T. Laaksonen, L.-S. Wang, T. Guo, P. Nordlander, and R. E. Smalley: Phys. Rev. B **51** (1995) 4668.
20) R. Georgiadis, E. R. Fisher, and P. B. Armentrout: J. Am. Chem. Soc. **111** (1989) 4251.
21) M. P. Irion, A. Selinger, and B. Bunsenges: Phys. Chem. Chem. Phys. **93** (1989) 1408.
22) W. D. Vann, R. C. Bell, and A. W. Castleman Jr.: J. Phys. Chem. A **103** (1999) 10846.
23) M. Ichihashi, T. Hanmura, R. T. Yadav, and T. Kondow: J. Phys. Chem. A **104** (2000) 11885.
24) T. Hanmura, M. Ichihashi, and T. J. Kondow: Phys. Chem. A **106** (2002) 4525.
25) S. Maruyama, L. R. Anderson, and R. E. Smalley: Rev. Sci. Instrum. **61** (1990) 3686.
26) M. Kohno, S. Inoue, A. Yabe, and S. Maruyama: Micro. Thermophys. Eng. **7** (2003) 33.
27) S. Maruyama, M. Kohno, and S. Inoue: Therm. Sci. Eng. **7** (1999) 69.

28) S. Maruyama, Y. Yamaguchi, M. Kohno, and T. Yoshida: Fullerene Sci. Technol. **7** (1999), 621.
29) A. G. Marshall: in *Fourier Transforms in NMR, Optical, and Mass Spectrometry*, ed. F. R. Verdun (Elsevier, Amsterdam, 1990).

Appendix A Hydrogen and Deuterium (H/D) Exchange Reaction

Detailed analyses of chemisorption experiments on ethanol-*d* (CH_3CH_2OD) in Fig. 7(b) and ethanol-d_6 (CD_3CD_2OD) in Fig. 7(d) are provided with the hydrogen and deuterium (H/D) exchange reaction using residual H_2 molecules in the ICR cell or from water molecules.

A-1. Reaction with ethanol-*d* (CH_3CH_2OD)

From Fig. 7(b), the 42 and 47 amu peaks from bare cluster are "dehydrogenated" and "simple chemisorption." According to our reaction model in Fig. 8, the dehydrogenated reaction is described as follows.

$$Co_n^+ + C_2H_5OD \rightarrow Co_n(C_2H_2O)^+ + H_2 + HD \qquad \text{(A1)}$$

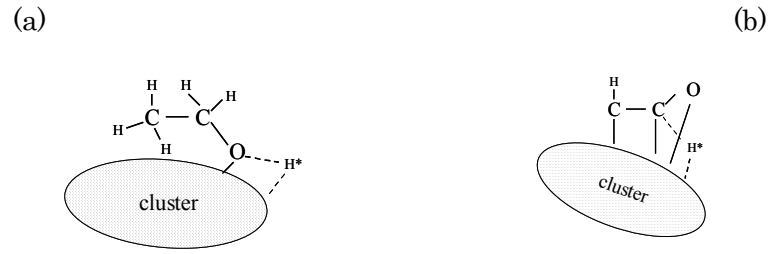

Fig. A1. H/D exchangeable sites. H* tends to be exchanged in (a) simple chemisorptions and (b) dehydrogenated chemisorptions.

The peak position of 42 amu from the bare cluster is consistent with this reaction. However, a small peak at 43 amu from the bare cluster is also distinguished. This peak can be explained by the exchange reaction of initially dissociated D atom with one H atom marked as H* in Fig. A1(b). On the other hand, there is also a signal at 46 amu from the bare cluster next to the simple-chemisorption peak marked as ■. We cannot understand this peak position within the framework of our reaction model in Fig. 8, and it is very difficult to imagine that only a hydrogen atom detaches a cluster. Hence, we assume the following H/D exchange reaction. In the first step of the chemisorption in Fig. 8(a), a deuterium atom is expected to be dissociated on the cluster. With collisions of background H_2 molecules, the H/D exchange reaction can happen as follows.

$$Co_n(C_2H_5OD)^+ + H_2 \rightarrow Co_n(C_2H_5OH)^+ + DH \quad \text{(A2)}$$

Even though under an ultrahigh vacuum condition at (1–2) × 10^{-8} Torr, considerable collisions with H_2 are expected.

A-2. Reaction with ethanol-d_6 (CD_3CD_2OD)

The same logic as that in Appendix A-1 can be applied for the reaction with ethanol-d_6 (CD_3CD_2OD) in Fig. 7(d). The H/D exchange reaction by collisions with background H_2 molecule is quite efficient as seen in the stronger 51 amu peak from the bare cluster compared with the 52 amu peak marked as ■. This can be explained by more dissociated D atoms during reactions in Figs. 8(a)-8(b). Because of these H atoms coming to the H* position in Fig. A1(b), the dehydrogenated product is $Co_n(CDCHO)^+$ and not $Co_n(CDCDO)^+$ as seen in the 43 amu peak from the bare cluster in Fig. 7(d).

Appendix B Intermediate Reaction of Dehydrogenation Process

Figure A2 shows the chemical reaction of Co_{16}^+ with ethanol-d_3 (CD_3CH_2OH). The weak signal at approximately 990 amu (46 amu from Co_{16}^+) is considered as an intermediate signal of the dehydrogenation process. Considering the mass difference, one hydrogen atom and one deuterium atom must have been dissociated and detached from this cluster. Here, assuming one atom dissociates from each carbon atom, one new chemical bond might arise between C1 and C2, as shown in Fig. 8.

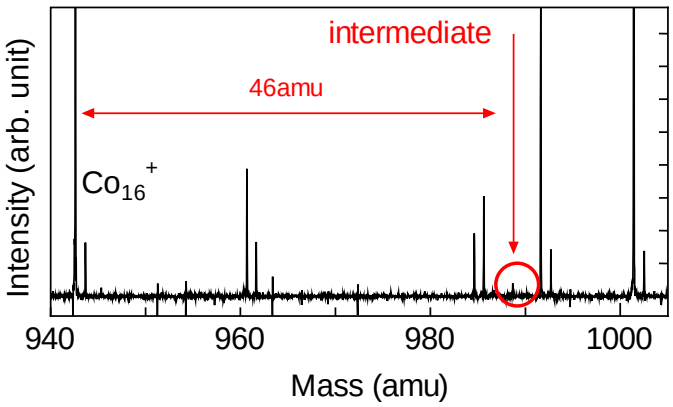

Fig. A2. Intermediate product observed in the reaction of Co_{16}^+ with ethanol-d_3 (CD_3CH_2OH).